

TMD gluon density in nuclei versus experimental data on heavy flavor production at LHC

A.V. Lipatov^{1,2}, M.A. Malyshev², A.V. Kotikov¹, X. Chen^{3,4}

December 4, 2023

¹*Joint Institute for Nuclear Research, 141980, Dubna, Moscow region, Russia*

²*Skobeltsyn Institute of Nuclear Physics, Lomonosov Moscow State University, 119991,
Moscow, Russia*

³*Institute of Modern Physics, Chinese Academy of Sciences, Lanzhou 730000, China*

⁴*School of Nuclear Science and Technology, University of Chinese Academy of Sciences,
Beijing 100049, China*

Abstract

Analytical expressions for the Transverse Momentum Dependent (TMD, or unintegrated) gluon and sea quark densities in nuclei are derived at leading order of QCD running coupling. The calculations are performed in the framework of the rescaling model and Kimber-Martin-Ryskin (KMR) prescription, where the Bessel-inspired behavior of parton densities at small Bjorken x values, obtained in the case of flat initial conditions in the double scaling QCD approximation, is applied. The derived expressions are used to evaluate the inclusive heavy flavor production in proton-lead collisions at the LHC. We find a good agreement of our results with latest experimental data collected by the CMS and ALICE Collaborations at $\sqrt{s} = 5.02$ GeV.

Keywords: heavy quarks, high-energy factorization, TMD gluon densities, Kimber-Martin-Ryskin approach, EMC effect

1 Introduction

It is well known that the usual concept of QCD factorization for proton-proton (pp) interactions assumes that the corresponding inclusive production cross section is calculated as a convolution of short-distance partonic cross sections and parton (quark or gluon) distribution functions in a proton (PDFs). Suggesting that there is no hot medium formed in proton-nucleus (pA) collisions, this concept is often extrapolated to pA interactions by replacing usual PDFs with nuclear PDFs (nPDFs) while keeping hard scattering cross sections the same (see, for example, [1–4]). However, some additional phenomena, so called cold nuclear matter effects¹, can affect this picture (see [5–8] and references therein). Detailed knowledge of nPDFs, in particular, gluon distribution in nuclei, is necessary for theoretical description of pA processes studied at modern (LHC, RHIC) and future colliders (FCC-he, EIC, EIC, NICA). Moreover, it is important in discriminating the initial nuclear effects from the subsequent hot medium effects essential for more complex nucleus-nucleus (AA) collisions, where nuclear matter can reach extremely high energy densities and temperatures, transforming into quark-gluon plasma (see also review [9] for more information). In this sense, production of charm and beauty flavors in pA interactions is of particular interest, because these processes directly probe the gluon distributions in the colliding particles.

Experimental investigation of deep inelastic scattering of leptons on nuclei performed by the European Muon Collaboration reveals the appearance of a significant nuclear effect [10], which excludes the naive idea of the nucleus as a system of quasi-free nucleons (see also [11, 12] for review). From theoretical point of view, there are two main scenarios to determine the nPDFs. In the first of them, nPDFs at some initial (or starting) scale μ_0^2 are extracted from global fits to nuclear data using empirical parametrization of their shape and normalizations (see, for example, [1–4] and references therein). Then, numerical solution of Dokshitzer-Gribov-Lipatov-Altarelli-Parisi (DGLAP) equations [13] is employed to describe the corresponding QCD evolution (dependence on the scale μ^2). An alternative approach is based on some nPDF models (see [14] for more information). Here we follow the rescaling model [15] based on the assumption that the effective size of gluon and quark confinement in the nucleus is greater than in the free nucleon [16]. Within the perturbative QCD, this confinement rescaling predicts that PDFs and nPDFs can be connected by scaling the argument μ^2 (see also review [17]). So that, the rescaling model demonstrates the features inherent in both approaches: there are certain relationships between conventional and nuclear PDFs that arise as a result of shifting the values of the scale μ^2 and, at the same time, both densities obey DGLAP equations. Initially, the rescaling model was proposed for the domain of valence quarks dominance, $0.2 \leq x \leq 0.8$, where x is the Bjorken variable. Later it was extended to small x [18, 19] (see also a short review [20]), where certain shadowing and antishadowing effects were found for gluon and sea quark distributions².

The main goal of our study is to derive analytical expressions (at leading order in the QCD coupling α_s) for the Transverse Momentum Dependent (TMD, or unintegrated) gluon and sea quark densities in nuclei (nTMDs) using the rescaling model [15] and popular Kimber-Martin-Ryskin (KMR) formalism [23] (see also [24]). These quantities encode nonperturbative information on hadron structure, including transverse momentum and polarization degrees of freedom. Currently they are widely used in a number of applications to topical issues in high energy physics phenomenology, especially for multi-scale

¹These are, for example, soft gluon interactions between hadrons in the initial and final states.

²Recently the rescaling model was applied to the lineally polarized gluon density in nuclei [21], see also [22].

or non-inclusive collider observables (see, for example, review [25] for more information). Next, the calculated TMD gluon density will be applied to investigate the heavy flavor (charm and beauty) production in proton-lead collisions at $\sqrt{s_{\text{NN}}} = 5.02$ TeV. Such processes are known to be sensitive to the gluon content of the nucleus and provide us with possibility to reconstruct the full map of the latter [26]. Of course, they are great of importance to first test of the derived expressions. We will use the k_T -factorization [27], or high-energy factorization [28] approach, which turns to be a convenient alternative to explicit higher-order pQCD calculations. In fact, a large piece of NLO + NNLO + ... corrections important at high energies can be effectively taken into account in the form of the TMD gluon density [25]. Our predictions are compared with latest experimental data taken by the CMS [29–31] and ALICE [32] Collaborations at the LHC. The consideration below extends and continues the line of our previous studies [21, 22, 33, 34].

The outline of our paper is following. In Section 2 we briefly describe our theoretical framework and basic steps of our calculation. In Section 3 we present the numerical results and discussion. Section 4 sums up our conclusions.

2 The model

This section provides a short description of the calculation steps for the TMD gluon and sea quark densities in a proton and nuclei and a brief review of the k_T -factorization formulas for heavy flavor production.

2.1 Conventional (collinear) PDFs in a proton

As it was argued [35], the HERA small- x data can be well interpreted in terms of so-called double asymptotic scaling approximation, which is related to the asymptotic behaviour of DGLAP evolution (see also [36–38]). In this approximation, flat initial conditions for conventional gluon and sea quark densities in a proton $f_a(x, \mu^2)$ at some scale Q_0^2 could be used: $f_a(x, Q_0^2) = A_a$, where $a = q$ or g [36, 37, 39]. At leading order (LO) of perturbative QCD, small- x expressions for $f_a(x, \mu^2)$ read³:

$$\begin{aligned} f_a(x, \mu^2) &= f_a^+(x, \mu^2) + f_a^-(x, \mu^2), \\ f_g^+(x, \mu^2) &= \left(A_g + \frac{4}{9} A_q \right) \bar{I}_0(\sigma) e^{-\bar{d}_+ s} + O(\rho), \quad f_g^-(x, \mu^2) = -\frac{4}{9} A_q e^{-d_- s} + O(x), \\ f_q^+(x, \mu^2) &= \frac{N_f}{3} \left(A_g + \frac{4}{9} A_q \right) \tilde{I}_1(\sigma) e^{-\bar{d}_+ s} + O(\rho), \quad f_q^-(x, \mu^2) = A_q e^{-d_- s} + O(x), \end{aligned} \quad (1)$$

where

$$\begin{aligned} s &= \ln \left(\frac{\alpha_s(Q_0^2)}{\alpha_s(\mu^2)} \right), \quad \sigma = 2 \sqrt{|\hat{d}_+ s| \ln \left(\frac{1}{x} \right)}, \quad \rho = \frac{\sigma}{2 \ln(1/x)}, \\ \hat{d}_+ &= -\frac{12}{\beta_0}, \quad \bar{d}_+ = 1 + \frac{20 N_f}{27 \beta_0}, \quad d_- = \frac{16 N_f}{27 \beta_0}, \end{aligned} \quad (2)$$

and $\bar{I}_\nu(\sigma)$ and $\tilde{I}_\nu(\sigma)$ are combinations of modified Bessel functions (at $s \geq 0$, i.e. $\mu^2 \geq Q_0^2$) and usual Bessel functions (at $s < 0$, i.e. $\mu^2 < Q_0^2$):

$$\tilde{I}_\nu(\sigma) = \begin{cases} \rho^\nu I_\nu(\sigma), & \text{if } s \geq 0; \\ (-\rho)^\nu J_\nu(\sigma), & \text{if } s < 0, \end{cases} \quad \bar{I}_\nu(\sigma) = \begin{cases} \rho^{-\nu} I_\nu(\sigma), & \text{if } s \geq 0; \\ \rho^{-\nu} J_\nu(\sigma), & \text{if } s < 0. \end{cases} \quad (3)$$

³The both leading and next-to-leading formulas and their derivation can be found [36, 39].

Here $N_f = 4$ is the number of active (massless) quark flavors and $\beta_0 = 11 - 2N_f/3$ is the first coefficient of the QCD β -function in the $\overline{\text{MS}}$ -scheme. The parameters A_a and Q_0^2 have been extracted [39] from a fit to HERA data on the proton structure function $F_2(x, Q^2)$ for $\alpha_s(M_Z^2) = 0.1168$ (see below).

2.2 Rescaling model and nuclear PDFs

In the rescaling model [15], the structure function $F_2^A(x, Q^2)$ and, consequently, the valence part $f_V^A(x, \mu^2)$ of the quark density in a nucleus A are modified at intermediate and large x values, $0.2 \leq x \leq 0.8$, as follows

$$f_V^A(x, \mu^2) = f_V(x, \mu_{A,V}^2), \quad (4)$$

where the new scale $\mu_{A,V}^2$ is related to μ^2 by [18]

$$s_V^A \equiv \ln \frac{\ln \mu_{A,V}^2 / \Lambda_{\text{QCD}}^2}{\ln Q_0^2 / \Lambda_{\text{QCD}}^2} = s + \ln(1 + \delta_V^A) \approx s + \delta_V^A. \quad (5)$$

So that, kernel modification of the main variable s defined in (2) depends on the μ^2 -independent parameter δ_V^A having small values [18].

Next, since rise of sea quark and gluon densities increases with increasing values of μ^2 , the small- x PDF asymptotics (1) were applied [18] to the small x region of the EMC effect. In fact, in the case of nuclei, the evolution scale is less than μ^2 , that can directly reproduce the shadowing effect observed in global fits. So, one can assume that

$$f_a^A(x, \mu^2) = f_a^{A,+}(x, \mu^2) + f_a^{A,-}(x, \mu^2), \quad f_a^{A,\pm}(x, \mu^2) = f_a^\pm(x, \mu_{A,\pm}^2), \quad (6)$$

where $f_a^\pm(x, \mu^2)$ are given by (1). Thus, there are two free parameters $\mu_{A,\pm}^2$ which should be determined from the analysis of experimental data for the EMC effect at low x . Corresponding values of s_\pm^A turned out to be

$$s_\pm^A \equiv \ln \frac{\ln \mu_{A,\pm}^2 / \Lambda_{\text{QCD}}^2}{\ln Q_0^2 / \Lambda_{\text{QCD}}^2} = s + \ln(1 + \delta_\pm^A), \quad (7)$$

where δ_\pm^A can be presented as [18]

$$-\delta_\pm^A = c_\pm^1 + c_\pm^2 A^{1/3} \quad (8)$$

and

$$\begin{aligned} c_+^1 &= -0.055 \pm 0.015, & c_+^2 &= 0.068 \pm 0.006, \\ c_-^1 &= 0.071 \pm 0.101, & c_-^2 &= 0.128 \pm 0.039. \end{aligned} \quad (9)$$

In particular, for ^{208}Pb we have $\delta_+^{\text{Pb}} = -0.34$ and $\delta_-^{\text{Pb}} = -0.78$.

2.3 Kimber-Martin-Ryskin approach

The KMR approach is a formalism to construct the TMD gluon and quark distributions from conventional (collinear) PDFs. The key assumption here is that the transverse momentum dependence of the parton densities enters only at the last of QCD evolution (namely, DGLAP). The KMR procedure is believed to take into account effectively the main part of next-to-leading logarithmic (NLL) terms $\alpha_s^n \ln^{n-1} \mu^2 / \Lambda_{\text{QCD}}^2$ compared to the

leading logarithmic approximation (LLA), where terms proportional to $\alpha_s^2 \ln^n \mu^2 / \Lambda_{\text{QCD}}^2$ are taken into account.

In the integral formulation of KMR approach, the TMD gluon and quark densities at the leading order⁴ of α_s can be written as [23]

$$f_a(x, \mathbf{k}_T^2, \mu^2) = \frac{\alpha_s(\mathbf{k}_T^2)}{2\pi\mathbf{k}_T^2} T_a(\mu^2, \mathbf{k}_T^2) \sum_{a'} \int_x^{1-\Delta(\mathbf{k}_T^2)} \frac{dz}{z} P_{aa'}^{(0)}(z) D_a\left(\frac{x}{z}, \mathbf{k}_T^2\right), \quad (10)$$

where $D_a(x, \mu^2) = f_a(x, \mu^2)/x$ are the conventional PDFs in a proton, $P_{aa'}^{(0)}(z)$ are the usual unregulated leading order DGLAP splitting functions and $a, a' = q$ or g . The Sudakov form factors $T_a(\mu^2, \mathbf{k}_T^2)$ enable one to include logarithmic loop corrections and have the following form

$$T_a(\mu^2, \mathbf{k}_T^2) = \exp \left\{ - \int_{\mathbf{k}_T^2}^{\mu^2} dp^2 \frac{\alpha_s(p^2)}{2\pi p^2} \sum_{a'} \int_0^{1-\Delta(p^2)} dz z P_{a'a}^{(0)}(z) \right\}. \quad (11)$$

The cut-off parameter $\Delta(\mathbf{k}_T^2) = |\mathbf{k}_T|/(\mu + |\mathbf{k}_T|)$ imply the angular-ordering constraint⁵ specifically to the last evolution step to regulate soft gluon singularities. Following [39], everywhere below we use the phenomenological infrared modification of QCD coupling which effectively increases its argument at small scales, namely, $\alpha_s(\mu^2) \rightarrow \alpha_s(\mu^2 + m_\rho^2)$, where m_ρ is the ρ meson mass ('freezing' treatment), see [40] and discussions therein.

2.4 Analytical expressions for TMDs and nTMDs

Using conventional PDFs given by (1) as an input for KMR procedure, one can derive the analytical expressions for TMD gluon and quark densities in a proton. After some algebra we have [33]

$$f_a(x, \mathbf{k}_T^2, \mu^2) = \frac{c_a \alpha_s(\mathbf{k}_T^2)}{\pi \mathbf{k}_T^2} T_a(\mu^2, \mathbf{k}_T^2) \times \\ \times \left[D_a(\Delta) f_a\left(\frac{x}{1-\Delta}, \mathbf{k}_T^2\right) + D_a^+ f_a^+\left(\frac{x}{1-\Delta}, \mathbf{k}_T^2\right) + D_a^- f_a^-\left(\frac{x}{1-\Delta}, \mathbf{k}_T^2\right) \right], \quad (12)$$

where

$$D_q(\Delta) = \ln\left(\frac{1}{\Delta}\right) - \frac{(1-\Delta)(3-\Delta)}{4}, \quad D_g(\Delta) = \ln\left(\frac{1}{\Delta}\right) - \frac{(1-\Delta)(13-5\Delta+4\Delta^2)}{12}, \\ D_q^-(\Delta) = -N_f \frac{(1-\Delta)}{18} (2-\Delta+2\Delta^2), \quad D_g^-(\Delta) = 0, \\ D_g^+ = \frac{1}{\bar{\rho}_g} - (1-\Delta) + \frac{(1-\Delta)^2}{4} + \frac{4}{81} N_f, \\ D_q^+ = \frac{9}{8} (1-\Delta) \left[\frac{2\Delta^2 - \Delta + 2}{\rho_a} - \frac{4\Delta^2 + \Delta + 13}{6} \right], \quad (13)$$

and

$$\frac{1}{\rho_g} = \frac{I_1(\sigma)}{\rho I_0(\sigma)} \Big|_{x \rightarrow x/(1-\Delta)}, \quad \frac{1}{\rho_q} = \frac{I_0(\sigma)}{\rho I_1(\sigma)} \Big|_{x \rightarrow x/(1-\Delta)}. \quad (14)$$

⁴The next-to-leading formulas can be found [24].

⁵Another choice, $\Delta(\mathbf{k}_T^2) = |\mathbf{k}_T|/\mu$, which corresponds to the strong ordering condition, is also used in applications.

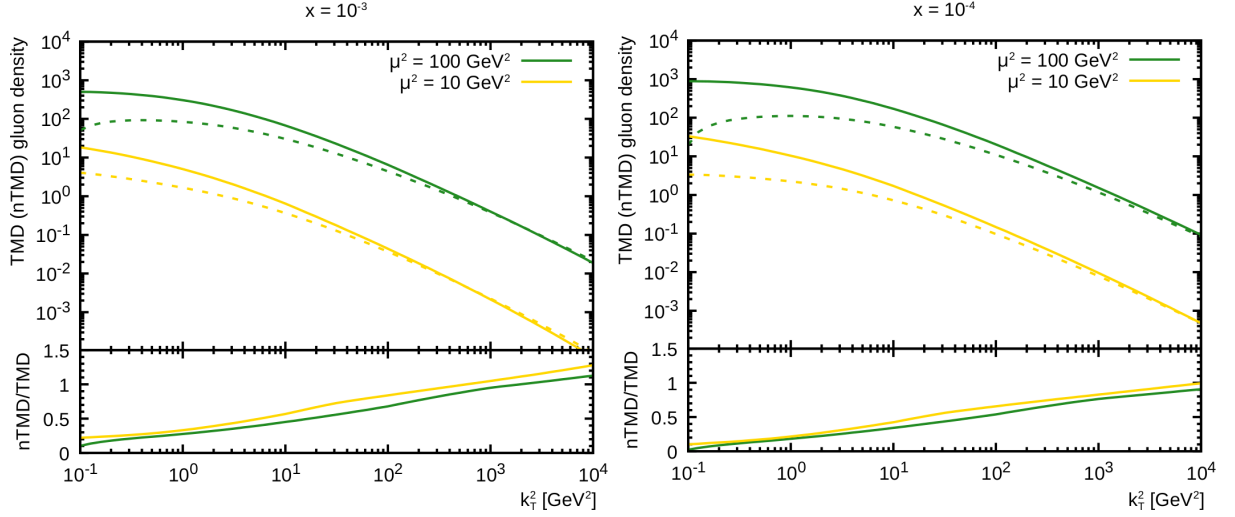


Figure 1: The TMD gluon densities in a proton (solid curves) and nuclei (dashed curves) calculated as a function of \mathbf{k}_T^2 for different values of x and μ^2 . Note that results for $\mu^2 = 100 \text{ GeV}^2$ are multiplied by a factor of 100. The ratios $f_g^A(x, \mathbf{k}_T^2, \mu^2)/f_g(x, \mathbf{k}_T^2, \mu^2)$ are presented also.

Here $c_g = C_A = N_c$, $c_q = C_F = (N_c^2 - 1)/(2N_c)$, $\Delta \equiv \Delta(\mathbf{k}_T^2)$ corresponds to the angular ordering constraint and 'frozen' treatment of QCD coupling is implied.

Following [33, 34], the analytic expression for TMD parton densities (12) has to be modified at large x in the form:

$$f_a(x, \mathbf{k}_T^2, \mu^2) \rightarrow f_a(x, \mathbf{k}_T^2, \mu^2) \left(1 - \frac{x}{1 - \Delta}\right)^{\beta_a(s)}, \quad \beta_a(s) = \beta(0) + \frac{4c_a s}{\beta_0}, \quad (15)$$

that is in agreement with similar modifications of conventional PDFs (see [18, 19] and references therein). The value of $\beta_a(0)$ can be estimated from the quark counting rules or extracted from the data. Below we set $\beta_g(0) = 3.03$, which was derived [33] from the best description of LHC data on inclusive b -jet production in pp collisions⁶.

Performing calculations in a similar way, for TMD gluon and sea quark densities in nuclei we have

$$f_a^A(x, \mathbf{k}_T^2, \mu^2) = \frac{c_a}{\pi \mathbf{k}_T^2} \left[\alpha_s(\mathbf{k}_{A,+}^2) (D_a(\Delta) + D_a^+) T_a(\mu^2, \mathbf{k}_{A,+}^2) f_a^{A,+} \left(\frac{x}{1 - \Delta}, \mathbf{k}_{A,+}^2 \right) + \right. \\ \left. + \alpha_s(\mathbf{k}_{A,-}^2) (D_a(\Delta) + D_a^-) T_a(\mu^2, \mathbf{k}_{A,-}^2) f_a^{A,-} \left(\frac{x}{1 - \Delta}, \mathbf{k}_{A,-}^2 \right) \right], \quad (16)$$

where $s \rightarrow s_{\pm}^A(\mathbf{k}_T^2)$ and $\mathbf{k}_{A,\pm}^2$ could be easily derived from

$$s_{\pm}^A(\mathbf{k}_T^2) \equiv \ln \frac{\ln \mathbf{k}_{A,\pm}^2 / \Lambda_{\text{QCD}}^2}{\ln Q_0^2 / \Lambda_{\text{QCD}}^2} = s + \ln(1 + \delta_{\pm}^A) = \ln \frac{\ln \mathbf{k}_T^2 / \Lambda_{\text{QCD}}^2}{\ln Q_0^2 / \Lambda_{\text{QCD}}^2} + \ln(1 + \delta_{\pm}^A). \quad (17)$$

The TMD gluon densities in a proton and nuclei calculated according to (12) and (16) with the 'frozen' scenario for strong coupling and appropriate treatment of $\beta_g(0)$ are shown in Fig. 1 as a function of gluon transverse momentum \mathbf{k}_T^2 for different values of x and hard scale μ^2 .

⁶The TMD gluon density in a proton given by (12) — (15) is available in the popular TMDLIB package [41] as KLSZ'2020 set.

2.5 Cross section of heavy flavor production

In the k_T -factorization approach, the heavy flavor production in pp or $p\bar{p}$ collisions is dominated by the direct leading-order off-shell gluon-gluon fusion subprocess

$$g^*(k_1) + g^*(k_2) \rightarrow Q(p_1) + \bar{Q}(p_2), \quad (18)$$

where $Q = c$ or b and four-momenta of corresponding particles are given in the parentheses. The contribution from the quark induced subprocesses is of almost no importance due to comparatively low quark densities. Corresponding cross section is calculated as a convolution of the off-shell (dependent on non-zero virtualities of the incoming gluons) partonic cross section and TMD gluon distribution in a proton [27, 28]. As it was already mentioned above, here we extend the consideration into pA collisions by employing the master factorization formula:

$$\sigma = \int \frac{dx_1}{x_1} \frac{dx_2}{x_2} \frac{d\phi_1}{2\pi} \frac{d\phi_2}{2\pi} d\mathbf{k}_{T1}^2 d\mathbf{k}_{T2}^2 f_g(x_1, \mathbf{k}_{T1}^2, \mu^2) f_g^A(x_2, \mathbf{k}_{T2}^2, \mu^2) d\hat{\sigma}^*(g^*g^* \rightarrow Q\bar{Q}), \quad (19)$$

where the initial off-shell gluons have fractions x_1 and x_2 of the parent proton and nucleus longitudinal momenta and azimuthal angles ϕ_1 and ϕ_2 . As usual, the off-shell partonic cross section reads

$$\begin{aligned} d\hat{\sigma}^*(g^*g^* \rightarrow Q\bar{Q}) &= \frac{(2\pi)^4}{2x_1x_2s} |\bar{\mathcal{A}}^2(g^*g^* \rightarrow Q\bar{Q})| \times \\ &\times \frac{d^3p_1}{(2\pi)^2 2p_1^0} \frac{d^3p_2}{(2\pi)^2 2p_2^0} \delta^{(4)}(k_1 + k_2 - p_1 - p_2). \end{aligned} \quad (20)$$

The analytic expression for the off-shell gluon-gluon fusion amplitude $|\bar{\mathcal{A}}^2(g^*g^* \rightarrow Q\bar{Q})|$ is known for quite a long time (see, for instance, [27, 28, 42]). Below we use it with the derived formulas (12) and (16) for TMD gluon densities in a proton and nuclei, respectively. In all other respect our calculation is generally identical to that performed previously [43].

3 Numerical results and discussion

We are now in a position to present our numerical results. First we describe our input and the kinematic conditions. After we fixed the TMD gluon densities in a proton and nuclei, the cross section (19) depends on the renormalization and factorization scales, μ_R and μ_F . We take them to be equal to transverse mass of the leading produced heavy quark, $\mu_R^2 = \mu_F^2 = \xi^2(m_Q^2 + \mathbf{p}_T^2)$, where the ξ parameter is altered from 1/2 to 2 around its default value of 1 to estimate theoretical uncertainties of our calculations. The quark masses are taken as $m_c = 1.4$ GeV and $m_b = 4.75$ GeV. The calculations were made with the one-loop formula for QCD coupling α_s with $\Lambda_{\text{QCD}} = 143$ MeV, $Q_0^2 = 0.43$ GeV² and $A_g = 0.77$, $A_q = 0.99$ [39, 44] for 'frozen' treatment of α_s . In case of heavy jet production, we fully associate the produced heavy quark with the final jet.

We start from charm and beauty jet production at proton-lead collisions at $\sqrt{s_{\text{NN}}} = 5.02$ TeV. The CMS data on c -jet transverse momentum spectra [31] refer to the pseudorapidity region (in nucleon-nucleon center-of-mass⁷ frame) of $|\eta_{\text{CM}}| < 1.5$. The data on b -jet production [30] were measured at four different pseudorapidity differences: $-2.5 < |\eta_{\text{CM}}| < -1.5$, $-1.5 < |\eta_{\text{CM}}| < -0.5$, $-0.5 < |\eta_{\text{CM}}| < 0.5$ and $0.5 < |\eta_{\text{CM}}| < 1.5$. Both

⁷The laboratory frame is defined with a shift of $\eta_{\text{lab}} = \eta_{\text{CM}} + 0.465$ with the positive direction corresponding to the proton beam direction.

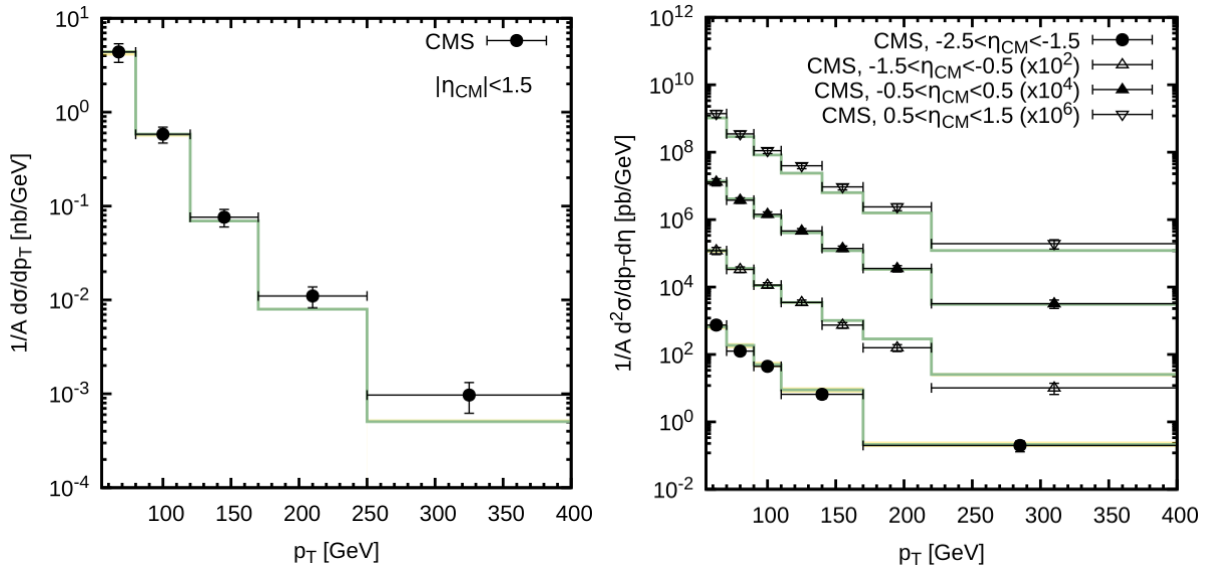


Figure 2: Differential cross sections of c (left) and b (right) jets production as functions of transverse momenta of the leading jet measured at $\sqrt{s_{\text{NN}}} = 5.02$ TeV. The uncertainty band corresponds to estimates made as described in the text. Experimental data are from [30,31].

these dataset correspond to jet transverse momentum $55 < p_T < 400$ GeV. Our predictions are shown in Fig. 2 in comparison with the CMS data [30,31]. The shaded bands (which, in fact, are quite narrow) represent our theoretical uncertainties estimated as discussed above. One can see that overall description of the data is reasonable good in all the pseudorapidity regions. The shape and absolute normalization of both measured charm and beauty jets are reproduced well, except, may be, last p_T bin ($p_T \sim 300$ GeV), where effects of parton showers and/or hadronization can play a role⁸.

To test lower transverse momenta we turn to data on D and B meson production in proton-lead collisions at the same energy. So, ALICE collaboration provided us with D^0 production data [32] measured in the kinematical region $0 < p_T < 24$ and $-0.96 < y_{\text{CM}} < 0.04$. The D^0 rapidity spectra were measured at three different regions of transverse momenta: $2 < p_T < 5$, $5 < p_T < 8$ and $8 < p_T < 16$ GeV, where rapidity region was extended then to $-1.265 < y_{\text{CM}} < 0.335$. The CMS data on B^+ meson production [29] were taken at $10 < p_T < 60$ GeV and $|y_{\text{lab}}| < 2.4$. To convert c or b quarks to D^0 or B^+ mesons we employ the standard Peterson fragmentation function with corresponding shape parameters $\epsilon_c = 0.06$ and $\epsilon_b = 0.006$, which are often used in the NLO pQCD calculations. Following to [45], we set branching ratios $B(c \rightarrow D^0) = 0.559$ and $B(b \rightarrow B^+) = 0.408$. The results of performed calculations are shown in Fig. 3. One can see that our predictions for all observables are consistent with the data within the theoretical and experimental uncertainties. There is only disagreement with the ALICE data on D^0 transverse momentum distribution at very low $p_T \leq m(D^0)$. However, we would like to point out that in order to obtain the reliable predictions at low p_T the large logarithmic terms $\sim \alpha_s^n \ln^n m_Q/p_T$ have to be resummed. It can be done using, for example, special soft gluon resummation technique [46, 47] or Collins-Soper-Sterman framework [48–50] (see also [25] for more information). This issue is not considered here. We note also that problematic low p_T region, $p_T \leq m(D^0)$, is excluded from D^0 rapidity measurements, see Fig. 3 (lower panels).

⁸Studying of these effects is out of range of the present paper.

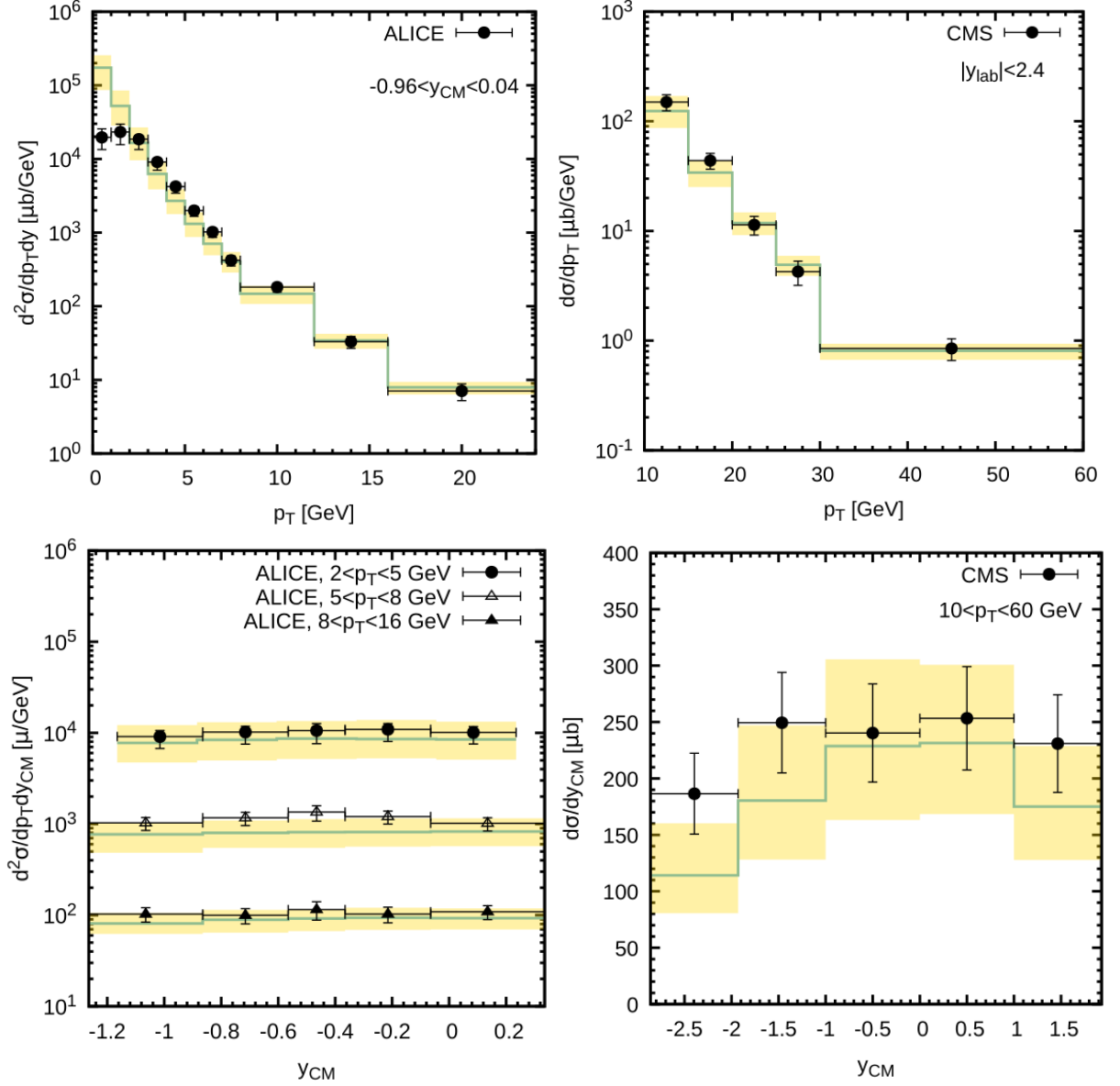


Figure 3: Differential cross sections of D^0 (left) and B^+ (right) jets production as functions of transverse momenta of the meson (upper panels) and their rapidity (lower panels) measured at $\sqrt{s_{\text{NN}}} = 5.02$ TeV. The uncertainty band corresponds to estimates made as described in the text. Experimental data are from [29, 32].

Process	experiment	theory
c -jet production	0.92 ± 0.13 [31]	$0.77^{+0.11}_{-0.07}$
b -jet production	1.22 ± 0.31 [30]	$0.82^{+0.14}_{-0.04}$
B^+ production	$1.11^{+0.38}_{-0.35}$ [29]	$0.77^{+0.02}_{-0.03}$

Table 1: Calculated nuclear modification factors R_{pA}^Q in comparison with the LHC data. The estimated theoretical uncertainties come from the scale variation as it is described in the text.

Another important observable is the nuclear modification factor R_{pA}^Q , describing the nuclear medium influence on the production dynamics:

$$R_{pA} = \frac{1}{A} \frac{\sigma(pA \rightarrow Q + X)}{\sigma(pp \rightarrow Q + X)}, \quad (21)$$

where $A = 208$ is the number of nucleons in the Pb nucleus. Our results for R_{pA}^Q (with $Q = c$ or b) are summarized in Table 1. All the estimated values are close to unity and our predictions agree with the experimental results within uncertainties.

Thus, our calculations show that the derived expressions for TMD gluon densities in a proton and nuclei provide a reasonably good description of LHC data for heavy flavor production in proton-lead collisions at the LHC, which is extremely sensitive to the gluon content of colliding particles. It is important for future investigations of proton-nucleus and nucleus-nucleus interactions in the TMD-based framework. Note that the consideration could be improved by taking into account Gross-Llewellyn-Smith and Gottfried sum rules for valence and nonsinglet quark distributions and momentum conservation for singlet quark and gluon densities similar to that as it was already done [44]. We plan to perform such derivation in a forthcoming study. Also we plan to incorporate the calculated nTMDs into the Monte-Carlo event generator PEGASUS [51] that significantly extends its feasibilities.

4 Conclusions

We have derived analytical expressions for the TMD gluon and sea quark densities in nuclei at leading order of QCD running coupling. The calculations are performed in the framework of the rescaling model and Kimber-Martin-Ryskin prescription, where the Bessel-inspired behavior of parton densities at small Bjorken x values, obtained in the case of flat initial conditions in the double scaling QCD approximation, is applied. Then we apply the obtained expressions to inclusive heavy flavor production in proton-lead collisions at the LHC, which is known to be sensitive to the gluon content of colliding particles. The calculations were performed in the framework of the k_T -factorization QCD approach and based on the dominating off-shell gluon-gluon fusion $g^*g^* \rightarrow Q\bar{Q}$ subprocess. The analysis covers the transverse momentum and rapidity spectra of charm and beauty jets as well as D^0 and B^+ mesons. We find a good agreement of our results with latest

experimental data collected by the CMS and ALICE Collaborations at $\sqrt{s} = 5.02$ GeV with the theoretical and experimental uncertainties. It is important for future studies of proton-nucleus and nucleus-nucleus interactions within the TMD-based approaches.

Acknowledgements

We thank S.P. Baranov for his interest, useful discussions and important remarks. Our study was in part supported by the Russian Science Foundation under grant 22-22-00387. The work of A.V.K. and A.V.L. was supported in part by the CAS President's International Fellowship Initiative.

References

- [1] K.J. Eskola, P. Paakkinen, H. Paukkunen, C.A. Salgado, *Eur. Phys. J. C* **82**, 413 (2022).
- [2] R.A. Khalek, R. Gauld, T. Giani, E.R. Nocera, T.R. Rabemananjara, J. Rojo, *Eur. Phys. J.C* **82**, 507 (2022).
- [3] K. Kovarik, A. Kusina, T. Jezo, D.B. Clark, C. Keppel, F. Lyonnet, J.G. Morfin, F.I. Olness, J.F. Owens, I. Schienbein, J.Y. Yu, *Phys. Rev. D* **93**, 085037 (2016).
- [4] P. Duwentäster, T. Jezo, M. Klasen, K. Kovarik, A. Kusina, K.F. Muzakka, F.I. Olness, R. Ruiz, I. Schienbein, J.Y. Yu, *Phys. Rev. D* **105** 114043, (2022).
- [5] J.-W. Qiu, I. Vitev, *Phys. Lett. B* **632**, 507 (2006).
- [6] H. Fujii, K. Watanabe, *Nucl.Phys. A* **920**, 78 (2013).
- [7] Z.-B. Kang, I. Vitev, E. Wang, H. Xing, C. Zhang, *Phys. Lett. B* **740**, 23 (2015).
- [8] B. Guiot, B.Z. Kopeliovich, *Phys. Rev. C* **102**, 045201 (2020).
- [9] A. Andronic, F. Arleo, R. Arnaldi, A. Beraudo, E. Bruna, D. Caffarri, Z. Conesa del Valle, J.G. Contreras, T. Dahms, A. Dainese, M. Djordjevic, E.G. Ferreira, H. Fujii, P.B. Gossiaux, R. Granier de Cassagnac, C. Hadjidakis, M. He, H. van Hees, W.A. Horowitz, R. Kolevator, B.Z. Kopeliovich, J.P. Lansberg, M.P. Lombardo, C. Lourenco, G. Martinez-Garcia, L. Massacrier, C. Mironov, A. Mischke, M. Nahrgang, M. Nguyen, J. Nystrand, S. Peigne, S. Porteboeuf-Houssais, I.K. Potashnikova, A. Rakotozafindrabe, R. Rapp, P. Robbe, M. Rosati, P. Rosnet, H. Satz, R. Schicker, I. Schienbein, I. Schmidt, E. Scomparin, R. Sharma, J. Stachel, D. Stocco, M. Strickland, R. Tieulent, B.A. Trzeciak, J. Uphoff, I. Vitev, R. Vogt, K. Watanabe, H. Woehri, P. Zhuang, *Eur. Phys. J. C* **76**, 107 (2016).
- [10] EMC Collaboration, *Phys. Lett. B* **123**, 275 (1983).
- [11] N.N. Nikolaev, *Sov. Phys. Usp.* **24**, 531 (1981);
V. Barone *et al.*, *Z. Phys. C* **58**, 541 (1993);
N.N. Nikolaev, B.G. Zakharov, *Z. Phys. C* **49**, 607 (1991).
- [12] M. Arneodo, *Phys. Rept.* **240**, 301 (1994);
P.R. Norton, *Rept. Prog. Phys.* **66**, 1253 (2003).

- [13] V.N. Gribov, L.N. Lipatov, Sov. J. Nucl. Phys. **15**, 438 (1972);
L.N. Lipatov, Sov. J. Nucl. Phys. **20**, 94 (1975);
G. Altarelli, G. Parisi, Nucl. Phys. B **126**, 298 (1977);
Yu.L. Dokshitzer, Sov. Phys. JETP **46**, 641 (1977).
- [14] S.A. Kulagin, Phys. Part. Nucl. **50**, 506 (2019);
S.A. Kulagin, EPJ Web Conf. **138**, 01006 (2017).
- [15] R.L. Jaffe *et al.*, Phys. Lett. B **134**, 449 (1984);
O. Nachtmann, H.J. Pirner, Z. Phys. C **21**, 277 (1984);
F.E. Close *et al.*, Phys. Rev. D **31** 1004, (1985).
- [16] F.E. Close, R.G. Roberts, G.G. Ross, Phys. Lett. B **129**, 346 (1983);
R.L. Jaffe, Phys. Rev. Lett. **50**, 228 (1983).
- [17] R.L. Jaffe, arXiv:2212.05616 [hep-ph].
- [18] A.V. Kotikov, B.G. Shaikhatdenov, P. Zhang, Phys. Rev. D **96**, 114002 (2017).
- [19] A.V. Kotikov, B.G. Shaikhatdenov, P. Zhang, Phys. Part. Nucl. Lett. **16**, 311 (2019) [1811.05615 [hep-ph]].
- [20] N.A. Abdulov, A.V. Kotikov, A.V. Lipatov, Phys. Part. Nucl. Lett. **20**, 557 (2023);
A.V. Kotikov, B.G. Shaikhatdenov, P. Zhang, EPJ Web Conf. **204**, 05002 (2019).
- [21] N.A. Abdulov, X. Chen, A.V. Kotikov, A.V. Lipatov, arXiv:2310.10496 [hep-ph].
- [22] N.A. Abdulov, X. Chen, A.V. Kotikov, A.V. Lipatov, arXiv:2310.08107 [hep-ph].
- [23] M.A. Kimber, A.D. Martin, M.G. Ryskin, Phys. Rev. D **63**, 114027 (2001);
G. Watt, A.D. Martin, M.G. Ryskin, Eur. Phys. J. C **31**, 73 (2003).
- [24] A.D. Martin, M.G. Ryskin, G. Watt, Eur. Phys. J. C **66**, 163 (2010).
- [25] R. Angeles-Martinez, A. Bacchetta, I.I. Balitsky, D. Boer, M. Boglione, R. Boussarie, F.A. Ceccopieri, I.O. Cherednikov, P. Connor, M.G. Echevarria, G. Ferrera, J. Grados Luyando, F. Hautmann, H. Jung, T. Kasemets, K. Kutak, J.P. Lansberg, A. Lelek, G.I. Lykasov, J.D. Madrigal Martinez, P.J. Mulders, E.R. Nocera, E. Petreska, C. Pisano, R. Placakyte, V. Radescu, M. Radici, G. Schnell, I. Scimemi, A. Signori, L. Szymanowski, S. Taheri Monfared, F.F. van der Veken, H.J. van Haevermaet, P. van Mechelen, A.A. Vladimirov, S. Wallon, Acta Phys. Polon. B **46**, 2501 (2015).
- [26] S.P. Baranov, H. Jung, A.V. Lipatov, M.A. Malyshev, Eur. Phys. J. C **77**, 2 (2017).
- [27] L.V. Gribov, E.M. Levin, M.G. Ryskin, Phys. Rep. **100**, 1 (1983);
E.M. Levin, M.G. Ryskin, Yu.M. Shabelsky, A.G. Shuvaev, Sov. J. Nucl. Phys. **53**, 657 (1991).
- [28] S. Catani, M. Ciafaloni, F. Hautmann, Nucl. Phys. B **366**, 135 (1991);
J.C. Collins, R.K. Ellis, Nucl. Phys. B **360**, 3 (1991).
- [29] CMS Collaboration, Phys. Rev. Lett. **116**, 032301 (2016).
- [30] CMS Collaboration, Phys. Lett. B **754**, 59 (2016).

- [31] CMS Collaboration, Phys. Lett. B **772**, 306 (2017).
- [32] ALICE Collaboration, Phys. Rev. Lett. **113**, 232301 (2014).
- [33] A.V. Kotikov, A.V. Lipatov, B.G. Shaikhatdenov, P. Zhang, JHEP **02**, 028 (2020).
- [34] A.V. Kotikov, A.V. Lipatov, P. Zhang, Phys. Rev. D **104**, 054042 (2021).
- [35] R.D. Ball, S. Forte, Phys. Lett. B **336**, 77 (1994).
- [36] A.V. Kotikov, G. Parente, Nucl. Phys. B **549**, 242 (1999).
- [37] A.Yu. Illarionov, A.V. Kotikov, G. Parente, Phys. Part. Nucl. **39**, 307 (2008).
- [38] L. Mankiewicz, A. Saalfeld, T. Weigl, Phys. Lett. B **393**, 175 (1997).
- [39] G. Cvetič, A.Yu. Illarionov, B.A. Kniehl, A.V. Kotikov, Phys. Lett. B **679**, 350 (2009).
- [40] B. Badelek, J. Kwiecinski, A. Stasto, Z. Phys. C **74**, 297 (1997);
A.V. Kotikov, A.V. Lipatov, N.P. Zotov, J.Exp.Theor.Phys. **101**, 811 (2005).
- [41] N.A. Abdulov, A. Bacchetta, S.P. Baranov, A. Bermudez Martinez, V. Bertone, C. Bissolotti, V. Candelise, L.I. Estevez Banos, M. Bury, P.L.S. Connor, L. Favart, F. Guzman, F. Hautmann, M. Hentschinski, H. Jung, L. Keersmaekers, A.V. Kotikov, A. Kusina, K. Kutak, A. Lelek, J. Lidrych, A.V. Lipatov, G.I. Lykasov, M.A. Malyshev, M. Mendizabal, S. Prestel, S. Sadeghi Barzani, S. Sapeta, M. Schmitz, A. Signori, G. Sorrentino, S. Taheri Monfared, A. van Hameren, A.M. van Kampen, M. Vanden Bemden, A. Vladimirov, Q. Wang, H. Yang, Eur. Phys. J. C **81**, 752 (2021).
- [42] N.P. Zotov, A.V. Lipatov, V.A. Saleev, Phys. Atom. Nucl. **66**, 755 (2003).
- [43] H. Jung, M. Kraemer, A.V. Lipatov, N.P. Zotov, JHEP **01**, 085 (2011);
H. Jung, M. Kraemer, A.V. Lipatov, N.P. Zotov, Phys. Rev. D **85**, 034035 (2012).
- [44] N.A. Abdulov, A.V. Kotikov, A.V. Lipatov, Particles **5**, 535 (2022).
- [45] PDG Collaboration, Prog. Theor. Exp. Phys. 2022, 083C01 (2022).
- [46] Yu.L. Dokshitzer, D. D'yakonov, S.I. Troyan, Phys. Lett. B **79**, 269 (1978).
- [47] G. Parisi, R. Petronzio, Nucl. Phys. B **154**, 427 (1979).
- [48] J.C. Collins, D.E. Soper, G.F. Sterman, Nucl. Phys. B **250**, 199 (1985);
J.C. Collins, D.E. Soper, Nucl. Phys. B **223**, 381 (1983).
- [49] J.C. Collins, D.E. Soper, Nucl. Phys. B **194**, 445 (1982);
J.C. Collins, D.E. Soper, Nucl. Phys. B **197**, 446 (1982).
- [50] R.D. Ball *et al.*, JHEP **04**, 040 (2015).
- [51] A.V. Lipatov, M.A. Malyshev, S.P. Baranov, Eur. Phys. J. C **80**, 330 (2020).